

# High-Harmonic Configurations of Cosmic Strings: An Analysis of Self-Intersections

Xavier A. Siemens<sup>a</sup> and T. W. B. Kibble<sup>a,b</sup>

<sup>a</sup>Blackett Laboratory, Imperial College, London SW7 2BZ, UK

<sup>b</sup>Isaac Newton Institute for Mathematical Sciences,  
20 Clarkson Road, Cambridge CB3 0EH, UK

## Abstract

A general formulation for describing odd-harmonic cosmic strings is developed and used to determine the self-intersection properties of high-harmonic loops. This is important because loop formation mechanisms produce high-harmonic components (kinks) which can only be eliminated very slowly by gravitational radiation, damping by the dense surrounding plasma in the era of string formation, or by the expansion of the Universe. For the class of loops examined it has been found that in the high-harmonic limit, essentially all cosmic loops self-intersect.

## 1 Introduction

Topological defects such as monopoles, cosmic strings and textures, are predicted by a number of grand unified theories as a result of symmetry breaking and may have important cosmological consequences [1]. Cosmic strings, in particular, could be responsible for the creation of the density fluctuations needed for large-scale structure formation [2, 3]. They are characterized by a tension or mass per unit length  $\mu$  which is related to the temperature  $T_{\text{GUT}}$  at which the phase transition takes place by  $\mu \sim T_{\text{GUT}}^2$ . Cosmic strings can meet and intercommute (exchange partners) or self-intersect. The latter process results in the formation of cosmic loops.

In the old cosmic string scenario [4, 5, 6] it was envisaged that these loops gave rise to the density fluctuations responsible for galaxy, galaxy cluster and supercluster formation. Loops decay primarily via gravitational radiation, giving them a very long lifetime. Recent numerical simulations of cosmic string networks [4, 7, 8, 9, 10], while confirming that a scaling solution is probably reached, have shown that there is a great deal of small-scale structure on the strings, and that the typical size of the loops formed is very small compared to the horizon. Since the lifetime of a loop is proportional to its length, this means that they do not live very long, and are unable to act as the seeds around which galaxies form. The dominant density perturbations must come from the long

strings. Nevertheless the loops could still have significant effects collectively. The extent to which they do so depends strongly on whether they typically break up into large numbers of small loops or reach a stable form that can survive a long time.

It is difficult to analyze the fate of such loops using the numerical simulations of cosmic string networks, because they lack the necessary resolution. Bennett and Bouchet [8] for example estimated that most loops break up into about ten stable daughter loops, but since the resulting stable loops are comparable in size to the resolution, it is unclear how far we should trust this conclusion. So it is desirable to study the evolution of loops analytically.

Several string parametrizations, corresponding to low harmonics (first and third), have been analyzed for self-intersections — those of Kibble and Turok [11], a one-parameter family of cosmic loops, Turok [12], with two parameters, Chen, DiCarlo and Hotes [13], with three and finally DeLaney, Engle and Scheick [14], with five. The principal justification for limiting study to such configurations (aside from computational convenience) is the argument that high-harmonic components are damped either by the expansion of the Universe, by friction with the dense surrounding plasma in the era immediately after string formation, or by the gravitational back-reaction, so that after a time loops become relatively smooth [12, 6, 13, 14]. However, we shall argue that these mechanisms may not in fact be so relevant to loop stability.

Figure 1: String intercommutation (a) and loop formation mechanisms: By the self-intersection of a long string (b) and by the self-intersection of a cosmic loop (c).

Loop formation mechanisms are illustrated in Figure 1. When strings meet they intercommute (Fig. 1(a)). Cosmic loops can be created by the self-intersection of a pre-existing loop (Fig. 1(b)) or of a long string (Fig. 1(b)). Both mechanisms inevitably produce kinks, or equivalently, high-harmonic components. Damping by interaction with the dense surrounding plasma only affects strings shortly after their initial formation. However, the loops of cosmological interest are produced when these effects are no longer important. Similarly, the expansion of the Universe is relevant only for loops comparable in size to the horizon, not to the small loops that dominate the recent loop distribution. High harmonics can also be radiated away by the emission of gravitational waves. The time scale of gravitational radiation effects, however, is very much larger than the period of oscillation of a cosmic loop. Therefore, since a cosmic loop in a self-intersecting trajectory will self-intersect within one oscillation period, it is reasonable to consider gravitational effects negligible as far as loop stability is concerned.

For all these reasons, it would seem therefore to be useful to investigate the properties of higher-harmonic cosmic loops to determine how the self-intersection probability varies with the number of harmonics. This is the problem we address in this work. The presence of these extra harmonics makes

the parameter space of cosmic loops larger and more complex than that of the string configurations analyzed so far.

Section 2 provides a summary of the string equations of motion and the general solutions in terms of Fourier series and in terms of the product of rotations [15]. Section 3 develops a general formulation for an odd-harmonic cosmic string in terms of the product representation, and describes our method for finding self-intersections. An explanation of how it is computationally implemented is given in an Appendix. In section 4 we describe the self-intersection results obtained for harmonic parametrizations which range from a 3/3 string (*i.e.*, one including up to the third harmonic on each of the left- and right-moving halves) up to a 41/41 string. We also discuss their sensitivity to different cutoffs. Finally, Section 5 contains a discussion of the new self-intersection results, their effect on galaxy-formation scenarios, and new directions of research.

## 2 Equations of Motion and General Solutions

The position of a string is described by  $x^\mu(\sigma, \tau)$ , where  $\sigma$  and  $\tau$  are the spacelike and timelike variables parametrizing the world sheet that the string sweeps out in space-time ( $c$  is taken to be 1). It is convenient to use the *orthonormal* (or *conformal*) gauge defined by the constraints [16]

$$\partial_\sigma x^\mu \partial_\tau x_\mu = \partial_\sigma x^\mu \partial_\sigma x_\mu + \partial_\tau x^\mu \partial_\tau x_\mu = 0. \quad (1)$$

For loops small compared with the horizon size and when gravitational radiation and external gravitational fields are considered negligible, the equation of motion of a cosmic string is the classical relativistic wave equation

$$\partial_\sigma^2 x^\mu - \partial_\tau^2 x^\mu = 0. \quad (2)$$

We are also free to impose the further condition  $x^0 = t$ , so that  $x^\mu(\sigma, t) = (t, \mathbf{r}(\sigma, t))$ . Then the solution in the centre of mass frame can be written

$$\mathbf{r}(\sigma, t) = \frac{1}{2}[\mathbf{a}(u) + \mathbf{b}(v)], \quad (3)$$

with

$$u = \sigma - t, \quad v = \sigma + t,$$

and the constraints become

$$\left[ \frac{d\mathbf{a}}{du} \right]^2 = \left[ \frac{d\mathbf{b}}{dv} \right]^2 = 1. \quad (4)$$

These vectors trace out closed loops on a unit sphere [11]. Here they will be referred to as the two halves of the string.

We can choose, for convenience, the period in  $\sigma$  to be  $2\pi$ . Thus  $\mathbf{r}$  is periodic in  $t$  with effective period  $\pi$ . The two halves of a closed string loop can be expanded in terms of the Fourier series

$$\begin{aligned} \mathbf{a}' &= \mathbf{Z} + \sum \mathbf{A}_n \cos(nu) + \sum \mathbf{B}_n \sin(nu), \\ \mathbf{b}' &= -\mathbf{Z} + \sum \mathbf{C}_n \cos(nv) + \sum \mathbf{D}_n \sin(nv), \end{aligned} \quad (5)$$

where  $\mathbf{a}'$  and  $\mathbf{b}'$  do not, in general, have the same number of harmonics. The linear centre of mass (c.m.) terms of  $\mathbf{a}$  and  $\mathbf{b}$  must be related due to spatial periodicity of closed loops. The problem therefore is reduced to finding a set of harmonic coefficients that satisfy the constraint equations (4) and the relation between the c.m. terms of  $\mathbf{a}$  and  $\mathbf{b}$  (5).

The general solution of an  $N$ -harmonic string half requires the satisfaction of  $4N + 1$  nonlinear relations between the vector coefficients. For the  $N=1$ ,  $N=2$  and  $N=3$  cases these relations can be solved with relative ease but for higher harmonics they become intractable. An alternative procedure is available involving products of rotations [15]. In terms of this representation a general  $N$ -harmonic string half is given by

$$\mathbf{c}'_N(u) = \rho_{N+1}R_z(u)\rho_N R_z(u)\dots\rho_3R_z(u)\rho_2R_z(u)\rho_1\hat{\mathbf{z}} \quad (6)$$

where

$$\rho_i = \rho(\theta_i, \phi_i) = R_z(-\theta_i)R_x(\phi_i)R_z(\theta_i), \quad (7)$$

and the rotation matrices are

$$R_z(u) = \begin{pmatrix} \cos u & -\sin u & 0 \\ \sin u & \cos u & 0 \\ 0 & 0 & 1 \end{pmatrix},$$

$$R_z(\theta) = \begin{pmatrix} \cos \theta & -\sin \theta & 0 \\ \sin \theta & \cos \theta & 0 \\ 0 & 0 & 1 \end{pmatrix},$$

and

$$R_x(\phi) = \begin{pmatrix} 1 & 0 & 0 \\ 0 & \cos \phi & -\sin \phi \\ 0 & \sin \phi & \cos \phi \end{pmatrix}.$$

It is clear that the magnitude of the vector remains fixed because all that is ever done is to rotate the original vector a certain number of times. The product representation is also complete but the proof of this is more involved and will not be included here for brevity (see Ref. [15]). It can be seen, however, that it exhibits the correct number of degrees of freedom. A general  $N$ -harmonic string half in terms of the Fourier series has  $6N + 3$  vector coefficients (Eq. 5) which must satisfy  $4N + 1$  nonlinear relations (Eq. 4) leaving a total of  $2N + 2$  independent degrees of freedom (Eq. 6). The ranges of the independent parameters  $\theta$  and  $\phi$  are polar-like and azimuthal-like respectively.

### 3 The General Odd-Harmonic String

The magnitude constraint has been solved by generating the string using the product of rotations. The relation between the centre of mass terms in the two string halves due to overall spatial periodicity of closed loops can be solved by taking an odd-harmonic string with no zeroth harmonic component. It should be noted that there are many other harmonic parametrizations with no zeroth harmonic. We have chosen the odd-harmonic string because it is the most

simple configuration of this type. With this procedure there will be a loss of generality — the loops have an extra inversion symmetry — but the problem of finding a set of parameters which satisfies the relation between the centre of mass terms of any two string halves in terms of the product representation resists analytical solution.

The odd  $N$ -harmonic string half is given by

$$\mathbf{c}'_N(u) = \rho_{N+2}R_z(2u)\rho_N R_z(2u) \dots R_z(2u)\rho_3 R_z(u)\rho_1 \hat{\mathbf{z}}, \quad (8)$$

where  $N$  is an odd integer. Because we want no zeroth harmonic component in the string we must take the angle  $\phi_1 = \pm \frac{\pi}{2}$  in both halves of the string. This gives a total of four families of strings per harmonic configuration just as found in Ref. [14] for the general three harmonic string. In this work we will only analyze those with  $\phi_1 = \frac{\pi}{2}$  in both halves of the string. For an  $N/M$  odd-harmonic string (the first letter denotes the number of harmonics of  $\mathbf{a}$  and the second that of  $\mathbf{b}$ ) this leaves us with a total of  $N + M + 4$  free parameters  $((N+2)+(M+2))$ . Two more parameters, the  $\theta_1$  for  $\mathbf{a}'$  and  $\mathbf{b}'$ , control the origin of  $u$  and  $v$  respectively and are set to  $-\frac{\pi}{2}$  to put the vector into standard form [15]. Because we are only looking for self-intersections we can eliminate three extra parameters from overall orientation freedom, namely  $\theta_{N+2}$  from  $\mathbf{a}'$  and  $\theta_{N+2}$  and  $\phi_{N+2}$  from  $\mathbf{b}'$  leaving  $R_x(\phi_{N+2})$  in  $\mathbf{a}'$  to ensure *relative* orientation freedom. This leaves a grand total of  $M + N - 1$  free parameters for the most general  $N/M$  odd harmonic cosmic loop with no zeroth harmonic. This result agrees with the number of string parameters of the 3/1 string presented in [13] and the 3/3 string presented in [14].

When all the redundant parameters have been eliminated the harmonic expansions in terms of the product of rotations for the two string halves are

$$\mathbf{a}'_N(u) = R_x(\phi_{N+2})R_z(2u)\rho_N R_z(2u) \dots R_z(2u)\rho_3 R_z(u)\hat{\mathbf{x}} \quad (9)$$

and

$$\mathbf{b}'_M(v) = R_z(2v)\rho_M R_z(2v) \dots R_z(2v)\rho_3 R_z(v)\hat{\mathbf{x}} \quad (10)$$

These formulae are the expressions for the derivatives of the string halves. What we need in order to find self-intersections, however, are the coefficients of the string halves themselves. Fortunately a recurrence relation developed in Ref. [15] can be used to compute the vector coefficients of the Fourier series in terms of the angles  $\theta_i$  and  $\phi_i$ . It yields the vector coefficients in standard form, so the coefficients of  $\mathbf{a}$  still need to be multiplied by  $R_x(\phi_{N+2})$ .

We have thus found a means of generating the vector coefficients of a general  $N/M$  odd-harmonic string which satisfies the magnitude and centre of mass constraints. This is the set of strings which we will analyze for self-intersections.

(a) (b)

Figure 2: Two examples of strings generated by the product of rotations and the recurrence relation: (a) A 19-19 harmonic string and (b) a 47-47 harmonic string.

The equation to be solved for finding self-intersections is

$$\mathbf{r}(\sigma, t) = \mathbf{r}(\sigma', t) \quad (11)$$

which in terms of the Fourier series is

$$\begin{aligned} & \sum \frac{1}{n} [\mathbf{A}_n \sin(nu) - \mathbf{B}_n \cos(nu) + \mathbf{C}_n \sin(nv) - \mathbf{D}_n \cos(nv)] \\ &= \sum \frac{1}{n} [\mathbf{A}_n \sin(nu') - \mathbf{B}_n \cos(nu') + \mathbf{C}_n \sin(nv') - \mathbf{D}_n \cos(nv')] \end{aligned} \quad (12)$$

where

$$u = \sigma - t, \quad v = \sigma + t, \quad (13)$$

$$u' = \sigma' - t, \quad v' = \sigma' + t, \quad (14)$$

and  $\sigma \neq \sigma' + 2n\pi$  for any integer  $n$ . This yields three non-linear equations in  $\sigma$ ,  $\sigma'$  and  $t$  to be solved simultaneously. Although individual cases of string parametrizations [11, 12, 13, 14, 17] have been solved analytically this problem is intractable for a general  $N/M$  odd-harmonic string. Numerically, however, it can be solved. The general procedure used here is described in the Appendix. To eliminate spurious intersections, it is necessary to introduce a small-distance cutoff. Self-intersection results are typically [13, 14] given as a function of the cutoff, and comparisons between them should only be made for the same cutoffs.

## 4 Self-Intersection Results

The Chen, DiCarlo, Hotes (CDH) string [13] has been used to test the correctness of the self-intersection method developed here. The percentage of self-intersections for the CDH string has been found to be  $33.6\% \pm 5\%$ . This result is in very good agreement with all the previous work [13, 14]. The Turok string [12, 13] has also been tested for self-intersections and a percentage of  $2\% \pm 1.25\%$  was found, which is in excellent agreement with the previous work as well. Furthermore, the 3/3 string presented here, which is equivalent to the DeLaney, Engle and Scheick (DES) string [14] has an intersection probability of about 0.6 (see Figures 3, 4 and 5), this is also consistent with their results. The self-intersection probabilities obtained for the generalized odd-harmonic strings are presented in the figures below. The parametrizations for which intersections have been calculated range from the 3/3 string to the 25/25 string for the smallest and largest cutoffs and from the 3/3 string to the 41/41 string for the middle cutoff.

A random flat parameter distribution has been used for the angles in the vector coefficients and the number of points  $K$  along the string was chosen to be  $K = 600$ , yielding a resolution  $\eta \approx 0.0104712$  radians which appears to be sufficient. Three different cutoffs have been used,  $\delta\sigma = |\sigma - \sigma'| = 0.084$  radians, 0.126 radians and 0.168 radians, corresponding to eight, twelve and sixteen step lengths, respectively. These are approximately the lower, middle and upper cutoffs used in the previous work on self-intersections thus allowing easy comparison. Each data point on the graphs is an average value of ten

Figure 3: Self-intersection probability as a function of the number of harmonics for a cutoff of  $\delta\sigma = |\sigma - \sigma'| = 0.084$  radians.

Figure 4: Self-intersection probability as a function of the number of harmonics for a cutoff of  $\delta\sigma = |\sigma - \sigma'| = 0.126$  radians.

samples of a hundred strings each. The errors are the standard deviation from the average of these ten samples.

In Figures 3, 4, and 5 plots are shown of the self-intersection probability as a function of the number of harmonics for the three cutoffs. It should be noted that the harmonic parametrization corresponding to a value  $N$  on the  $x$ -axis on the figures corresponds to a  $N/N$  harmonic string. The only parametrizations analyzed in this work correspond to strings with the *same* number of harmonics in each half.

In Figure 6 a plot of the logarithm of the stability probability as a function of the number of harmonics for the three cutoffs is presented. The stability probability is defined as the probability that loop will not self intersect (i.e.  $p_{\text{stab}} = 1 - p_{\text{SI}}$ ). The last six points do not have errorbars due to the fact that the lower value of the error is at infinity. As can be seen the stability probability  $p_{\text{stab}}$  can be fitted quite well to an exponential curve. The dashed curve on the plot is given by

$$p_{\text{stab}} = e^{\alpha + \beta N} \quad (15)$$

with parameters  $\alpha = -0.4$  and  $\beta = -0.2$ . The continuous curve is

$$p_{\text{stab}} = N^\delta e^{\gamma + \kappa N} \quad (16)$$

with parameters  $\delta = -0.2$ ,  $\gamma = -0.4$  and  $\kappa = -0.14$ , where  $N$  is the number of harmonics. It is clear that in the high harmonic limit all loops will self-intersect.

## 5 Discussion and Conclusions

We have set out to examine the self-intersection properties of high-harmonic cosmic loops. After the very early stages of string formation, damping by the dense surrounding plasma, by the expansion of the Universe, or by the emission of gravitational radiation does not have significant effects on the time scale of

Figure 5: Self-intersection probability as a function of the number of harmonics for a cutoff of  $\delta\sigma = |\sigma - \sigma'| = 0.168$  radians.

Figure 6: Plot of the logarithm of the stability probability as a function of the number of harmonics for the three cutoffs. The strings plotted here are the same as in the previous figures.

the order of the oscillation period. Consequently, these processes are irrelevant to the question of how many loops self-intersect.

We have found the most general  $N/M$  odd-harmonic string in terms of the product of rotations and devised a means for finding self-intersections. The results agreed with all previous work on the subject, but extended it to much higher harmonics. We have systematically analyzed the resulting string configurations to find the intersection probability in the high-harmonic limit. We have found that as a function of the number of harmonics the intersection probability is well described by an exponential. In the high-harmonic limit almost all loops self-intersect.

Although loops have been found not to be as important for structure formation in recent numerical simulations of cosmic string networks as was once thought, they may still have significant effects, on the density perturbations [3], on the microwave background [18], on the gravity-wave background [19], and possibly on the baryon asymmetry [20]. On the basis of our results, it appears that cosmic loops formed *after* the initial string formation era by the mechanisms described in Section 1 will almost all self-intersect within the first period of oscillation. As a result of the intersection process two or more kinky daughter loops are produced and, by the same line of reasoning, it is extremely probable that the daughter loops will re-intersect. It is not certain how far this process will go, but it seems likely to continue until the resulting loops have only a very few kinks, by which time they will be extremely small. Clearly it would be desirable to follow the evolution of the loops through several generations to see whether they continue to divide. Work in this direction is in progress. Bennett and Bouchet [8, 9] and Allen and Shellard [10] found in their simulations that the size of most of their child loops was determined by the resolution of their simulations, *i.e.*, close enough to the lower cutoff on loop size to suppress the chances of further division. In this work we have formulated loop trajectories analytically in an attempt to complement the numerical simulations made so far. We believe our method can provide a more definite answer to the question of the fate of cosmic string loops.

At birth, the loops are already fairly small compared to the horizon. A sequence of self-intersection processes will turn the initial parent loop into tiny loops, with very short lifetimes, so that they will decay into relativistic particles within a relatively short period of time. This is likely to reduce many of the observable effects of loops, in particular their effects on density perturbations, on the microwave background and on the gravitational-wave background. But it might enhance the effect on the baryon asymmetry.



## Appendix

Here we describe the implementation of our analysis.

When the number of harmonics for each half of the string has been selected, a set of string coefficients is randomly generated using the recurrence relation mentioned in Section 3. The number  $K$  of points along the string must be chosen. It determines the resolution  $\eta$  of the string in  $\sigma$  and  $t$ , via  $\eta = 2\pi/K$ . For consistency the resolution in  $\sigma$  and  $t$  should be the same. It should be small enough to ensure that the small scale detail of the loop is not lost.

The string is then time evolved for the given number of timesteps  $K/2$ , with  $t$  ranging from 0 to  $\pi$ , the effective period. At each timestep  $t_i$ , we search for self-intersections by expanding the equations (12) to first order about every pair of points  $u_j, v_j$  and  $u_k, v_k$  given by

$$\begin{aligned} u_j &= \sigma_j - t_i, & v_j &= \sigma_j + t_i, \\ u_k &= \sigma_k - t_i, & v_k &= \sigma_k + t_i, \end{aligned}$$

where  $j$  ranges<sup>1</sup> from 1 to  $K/2$ , and  $k$  from  $j$  to  $K/2$  and from  $j + K/2$  to  $K$ , as follows

$$\begin{aligned} & \sum \frac{1}{n} \left\{ \mathbf{A}_n [\sin(nu_j) + n \cos(nu_j)(u - u_j)] - \mathbf{B}_n [\cos(nu_j) - n \sin(nu_j)(u - u_j)] \right. \\ & \quad \left. + \mathbf{C}_n [\sin(nv_j) + n \cos(nv_j)(v - v_j)] - \mathbf{D}_n [\cos(nv_j) - n \sin(nv_j)(v - v_j)] \right\} \\ &= \sum \frac{1}{n} \left\{ \mathbf{A}_n [\sin(nu_k) + n \cos(nu_k)(u' - u_k)] - \mathbf{B}_n [\cos(nu_k) - n \sin(nu_k)(u' - u_k)] \right. \\ & \quad \left. + \mathbf{C}_n [\sin(nv_k) + n \cos(nv_k)(v' - v_k)] - \mathbf{D}_n [\cos(nv_k) - n \sin(nv_k)(v' - v_k)] \right\}. \end{aligned}$$

Substituting for  $u, v, u',$  and  $v'$  from (14) and rearranging the terms yields

$$\begin{aligned} & \sigma \sum \left\{ \mathbf{A}_n \cos(nu_j) + \mathbf{B}_n \sin(nu_j) + \mathbf{C}_n \cos(nv_j) + \mathbf{D}_n \sin(nv_j) \right\} \\ & - \sigma' \sum \left\{ \mathbf{A}_n \cos(nu_k) + \mathbf{B}_n \sin(nu_k) + \mathbf{C}_n \cos(nv_k) + \mathbf{D}_n \sin(nv_k) \right\} \\ & + t \sum \left\{ -\mathbf{A}_n [\cos(nu_j) - \cos(nu_k)] - \mathbf{B}_n [\sin(nu_j) - \sin(nu_k)] \right. \\ & \quad \left. + \mathbf{C}_n [\cos(nv_j) - \cos(nv_k)] + \mathbf{D}_n [\sin(nv_j) - \sin(nv_k)] \right\} \\ &= - \sum \left\{ \mathbf{A}_n \left[ \left( \frac{1}{n} \sin(nu_j) - u_i \cos(nu_j) \right) - \left( \frac{1}{n} \sin(nu_k) - u_j \cos(nu_k) \right) \right] \right. \\ & \quad - \mathbf{B}_n \left[ \left( \frac{1}{n} \cos(nu_j) + u_j \sin(nu_j) \right) - \left( \frac{1}{n} \cos(nu_k) + u_k \sin(nu_k) \right) \right] \\ & \quad \left. + \mathbf{C}_n \left[ \left( \frac{1}{n} \sin(nv_j) - v_j \cos(nv_j) \right) - \left( \frac{1}{n} \sin(nv_k) - v_k \cos(nv_k) \right) \right] \right\} \end{aligned}$$

---

<sup>1</sup>The symmetry of this set of strings is such that an intersection found at a point  $\sigma_i$  on the string will mean that there is another intersection at  $\sigma_i + \pi$ , so we only need to search for self-intersections in half the total range in  $\sigma$ .

$$-\mathbf{D}_n \left[ \left( \frac{1}{n} \cos(nv_j) + v_i \sin(nv_j) \right) - \left( \frac{1}{n} \cos(nv_k) + v_j \sin(nv_k) \right) \right] \Bigg\}.$$

As can be seen this is a linear system of three equations and three unknowns  $\sigma$ ,  $\sigma'$  and  $t$ , which is readily solvable by Cramer's rule. An intersection is found when the conditions  $|t_i - t| < \eta/2$ ,  $|\sigma_j - \sigma| < \eta/2$  and  $|\sigma_k - \sigma'| < \eta/2$  are satisfied. This makes the choice of resolution crucial to the accuracy of our results. The process is systematically repeated for every timestep until an intersection is found.

To avoid trivial solutions (*i.e.*,  $\sigma = \sigma'$ ) a cutoff  $\delta\sigma$  has been introduced. This means that if an intersection occurs at  $\sigma_j$  and  $\sigma_k$  with  $|\sigma_j - \sigma_k|$  smaller than the cutoff it is neglected. In practice, the Taylor expansion is not made for pairs of points for which  $|\sigma_j - \sigma_k| < \delta\sigma$ .

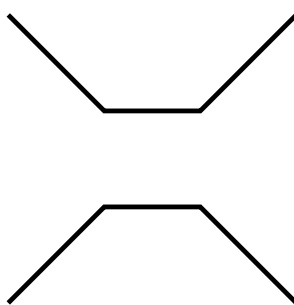
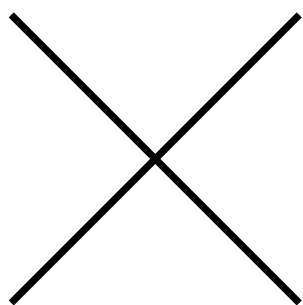
## References

- [1] T.W.B. Kibble, J. Phys. A 9 (1976) 1387; Phys. Rep. 67 (1980) 183.
- [2] Ya. B. Zel'dovich, Mon. Not. R. Astron. Soc. 192 (1980) 663;  
A. Vilenkin, Phys. Rev. Lett. 46 (1981) 1169; 1496(E); Phys. Rev. D 24 (1981) 2082.
- [3] T. Vachaspati and A. Vilenkin, Phys. Rev. Lett. 67 (1990) 1057;  
A. Albrecht and A. Stebbins, Phys. Rev. Lett. 68 (1990) 2121; 69 (1992) 2615.
- [4] A. Albrecht and N. Turok, Phys. Rev. Lett. 54 (1985) 1868.
- [5] A. Vilenkin, Phys. Rep. 121 (1985) 263;  
N. Turok, Phys. Rev. Lett. 55 (1985) 1801.
- [6] D.P. Bennett, Phys. Rev. D33 (1986) 872; Phys. Rev. D 34 (1986) 3592.
- [7] A. Albrecht and N. Turok, Phys. Rev. D 40 (1989) 973.
- [8] D.P. Bennett and F.R. Bouchet, Phys. Rev. Lett. 60 (1988) 257.
- [9] D.P. Bennett and F.R. Bouchet, Phys. Rev. Lett. 63 (1989) 2776; Phys. Rev. D 41 (1990) 2408;  
F.R. Bouchet and D.P. Bennett, Astrophys. J. 354 (1990) L41.
- [10] B. Allen and E.P.S. Shellard, Phys. Rev. Lett. 64 (1990) 119;  
E.P.S. Shellard and B. Allen, The Formation and Evolution of Cosmic Strings, eds. G.W. Gibbons, S.W. Hawking and T. Vachaspati (Cambridge University Press, Cambridge, 1990), p. 421.
- [11] T.W.B. Kibble and N. Turok, Phys. Lett. 116B (1982) 141.
- [12] N. Turok, Nucl. Phys. B 242 (1984) 520.
- [13] A. L. Chen, D. A. DiCarlo and S. A. Hotes, Phys. Rev. D 37 (1988) 863.
- [14] D. DeLaney, K. Engle and X. Scheick, Phys. Rev. D 41 (1990) 1775.

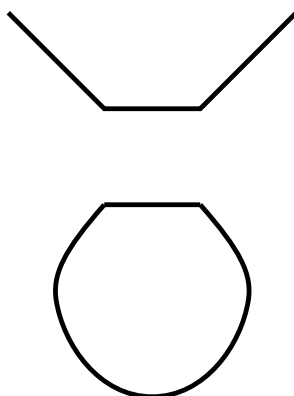
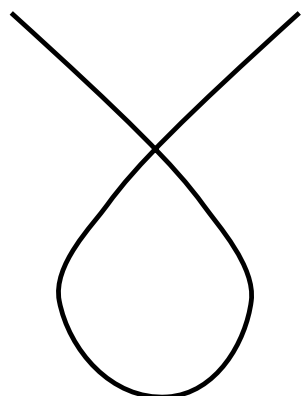
- [15] R.W. Brown and D.B. DeLaney, Phys. Rev. Lett. 63 (1991) 1674;  
R.W. Brown, M.E. Convery and D.B. DeLaney, J. Math. Phys. 32 (7) (1991) 1674.
- [16] P. Goddard, J. Goldstone, C. Rebbi and C.B. Thorn, Nucl.Phys. B 56 (1973) 109.
- [17] D. Garfinkle and T. Vachaspati, Phys. Rev. D 36 (1987) 2229.
- [18] D.P. Bennett, A. Stebbins and F.R. Bouchet, Atrophys. J. 399 (1992) L5;  
D. Coulson, P. Ferreira, P. Graham and N. Turok, Nature 368 (1994) 27
- [19] C. Hogan and M. Rees, Nature 311 (1984) 109;  
R. Caldwell and B. Allen, Phys. Rev. D 45 (1992) 3447;  
D.P. Bennett and F.R. Bouchet, Phys. Rev. D 43 (1991) 2733.
- [20] R.H. Brandenburger, A.C. Davis and M.B. Hindmarsh, Phys. Lett. 284B (1992) 81;  
A.C. Davis and M.A. Earnshaw, Phys. Lett. 394B (1993) 21.

This figure "fig1-1.png" is available in "png" format from:

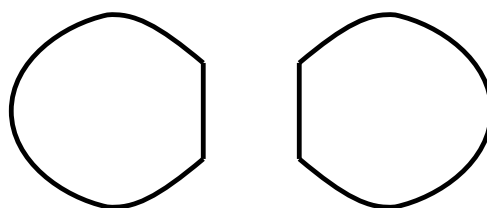
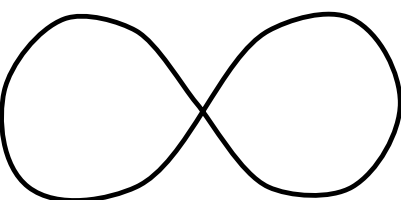
<http://arxiv.org/ps/hep-ph/9412216v2>



(a)



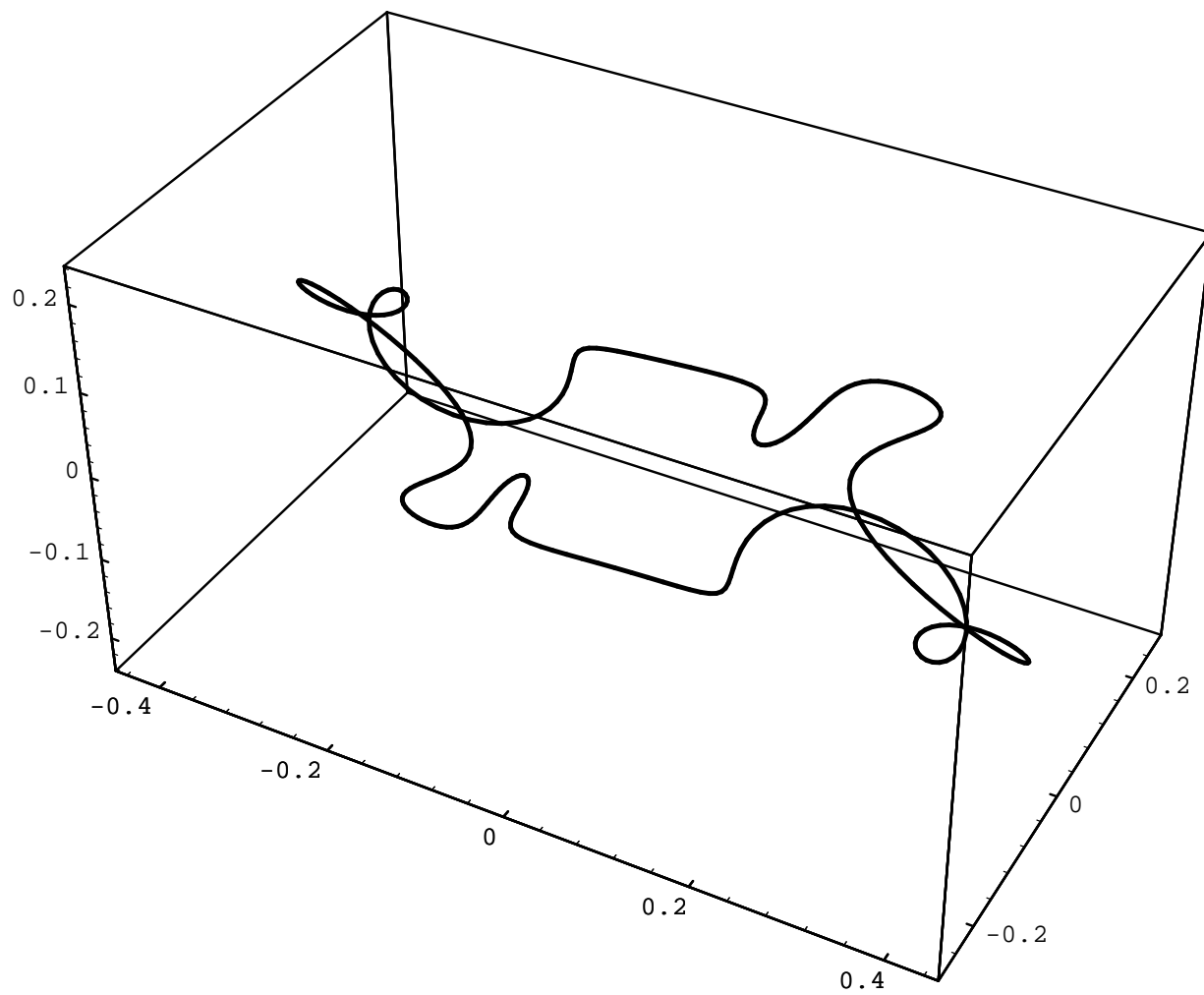
(b)

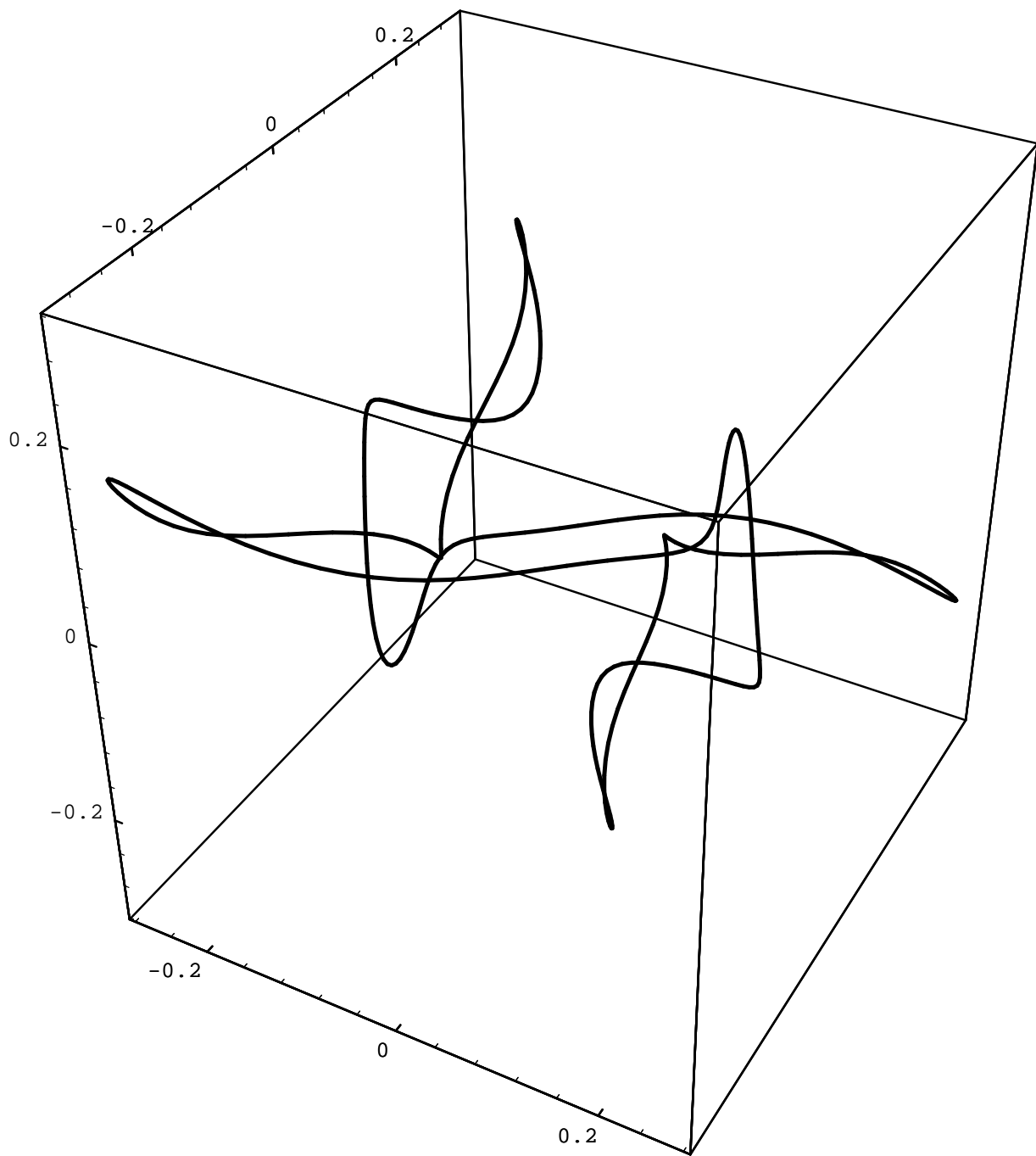


(c)

This figure "fig1-2.png" is available in "png" format from:

<http://arxiv.org/ps/hep-ph/9412216v2>

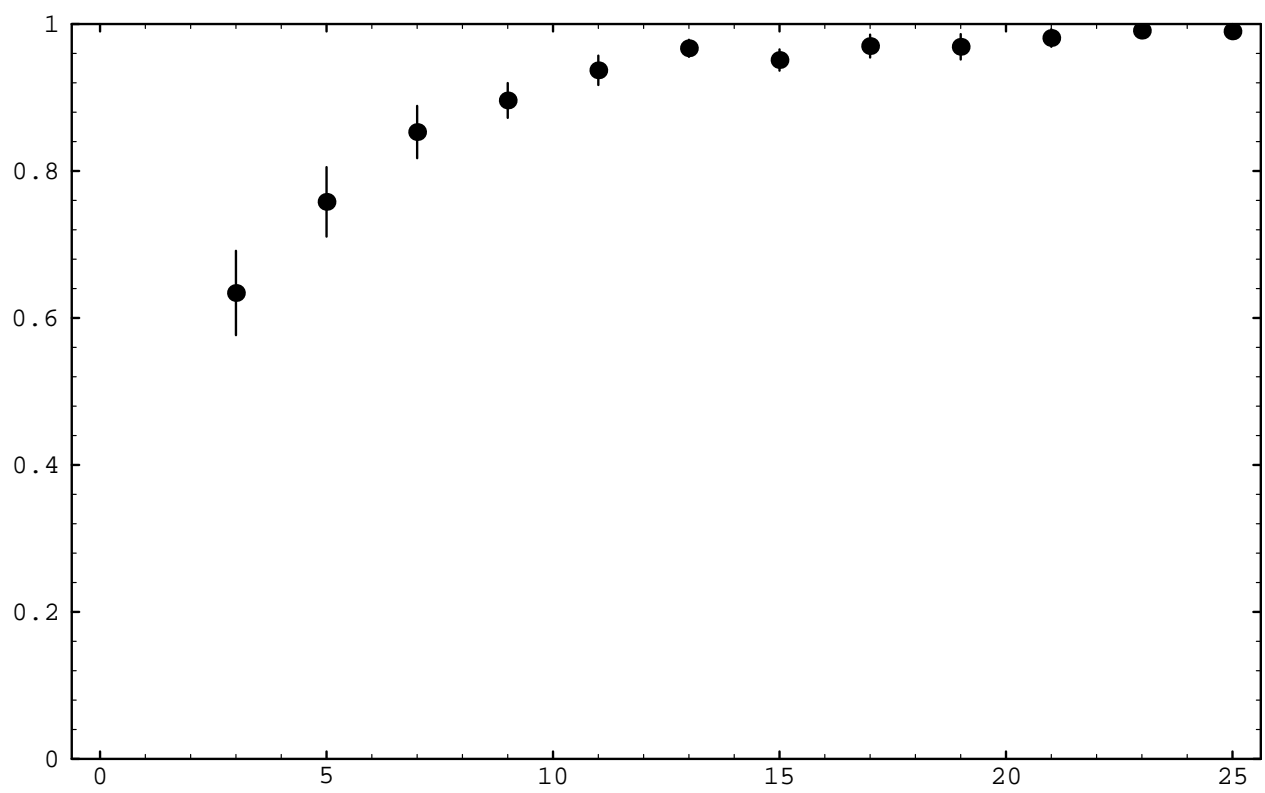






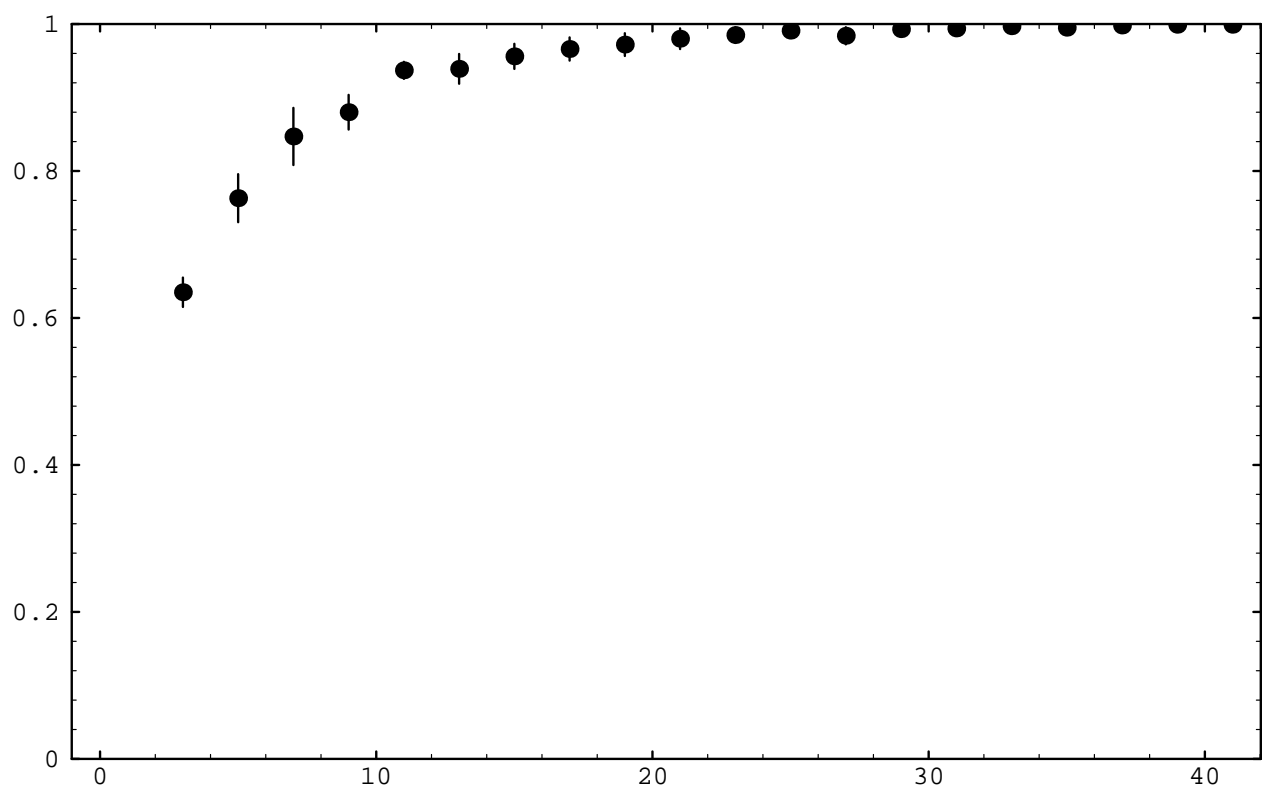
This figure "fig1-3.png" is available in "png" format from:

<http://arxiv.org/ps/hep-ph/9412216v2>



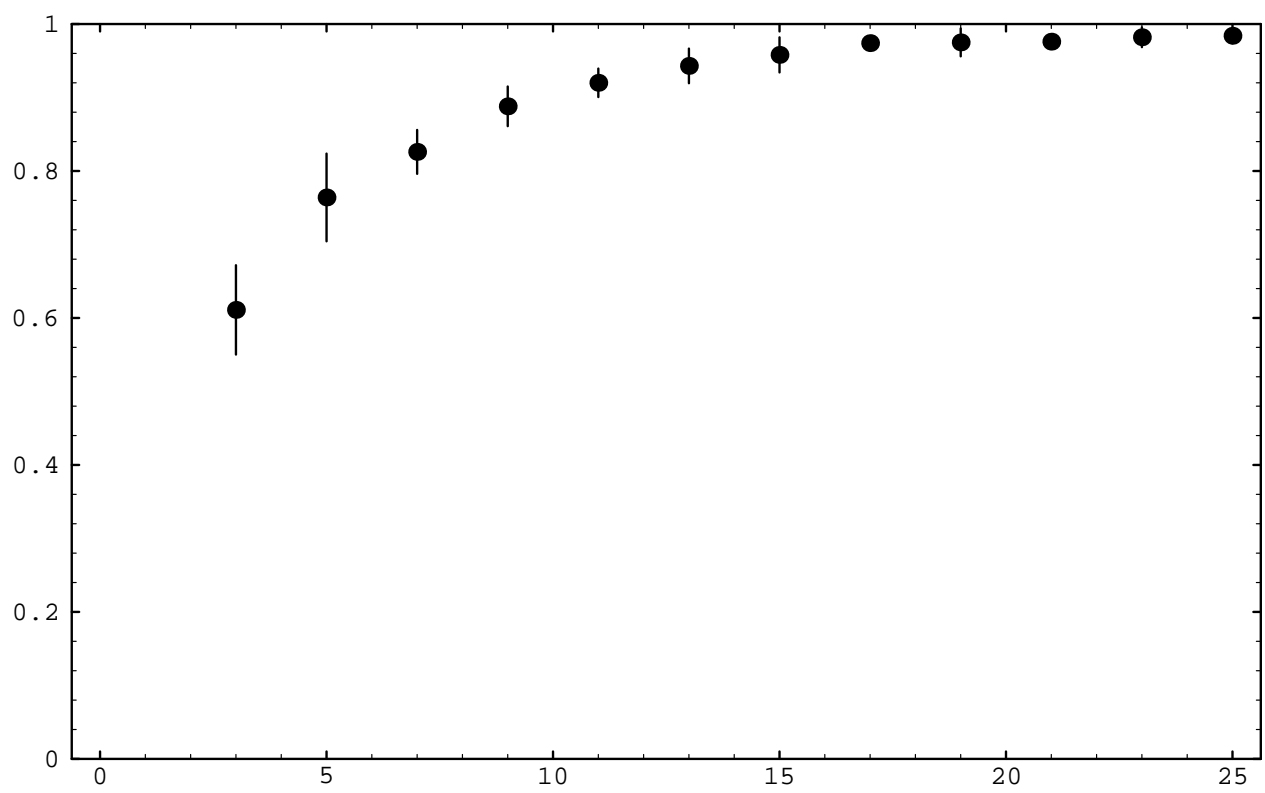
This figure "fig1-4.png" is available in "png" format from:

<http://arxiv.org/ps/hep-ph/9412216v2>



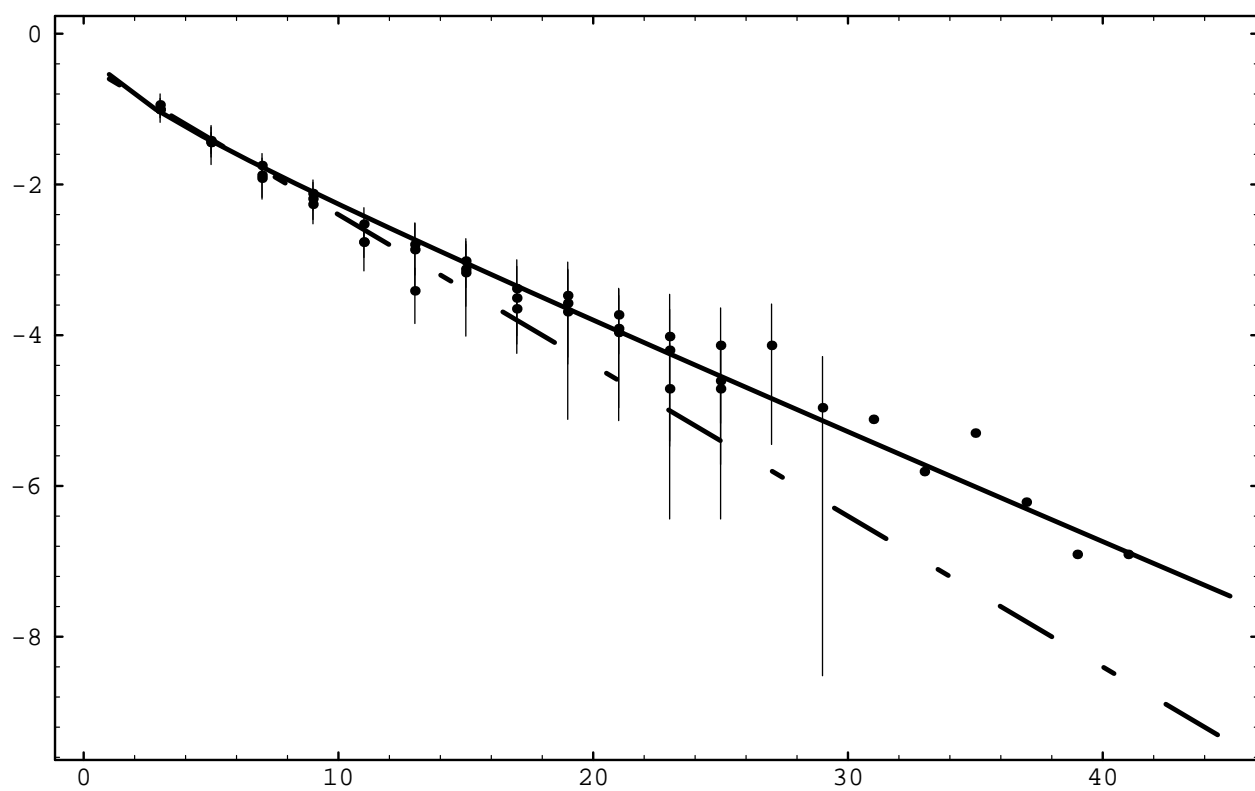
This figure "fig1-5.png" is available in "png" format from:

<http://arxiv.org/ps/hep-ph/9412216v2>



This figure "fig1-6.png" is available in "png" format from:

<http://arxiv.org/ps/hep-ph/9412216v2>





This figure "fig1-7.png" is available in "png" format from:

<http://arxiv.org/ps/hep-ph/9412216v2>